Force-induced growth of adhesion domains is controlled by receptor mobility

Ana-Sunčana Smith*[†‡], Kheya Sengupta[§¶], Stefanie Goennenwein[‖], Udo Seifert*, and Erich Sackmann[‖]

*II. Institut für Theoretische Physik II, Universität Stuttgart, Pfaffenwaldring 57/III, D-70550 Stuttgart, Germany; [†]Institut für Theoretische Physik I, Universität Erlangen-Nürnberg, Staudtstrasse 7, D-91058 Erlangen, Germany; [§]Institut für Bio- und Nanosysteme-4: Biomechanik, Forschungszentrum Jülich, Leo Brand Strasse, D-52425 Jülich, Germany; [¶]Centre de Recherche en Matière Condensée et Nanosciences, Centre National de la Recherche Scientifique, Campus de Luminy, Case 913, F-13288 Marseille Cedex 9, France; and [‖]E22 Institut für Biophysik, Technische Universität München, James Franck Strasse, D-85748 Garching, Germany

Communicated by L. B. Freund, Brown University, Providence, RI, March 10, 2008 (received for review October 13, 2007)

In living cells, adhesion structures have the astonishing ability to grow and strengthen under force. Despite the rising evidence of the importance of this phenomenon, little is known about the underlying mechanism. Here, we show that force-induced adhesion-strengthening can occur purely because of the thermodynamic response to the elastic deformation of the membrane, even in the absence of the actively regulated cytoskeleton of the cell, which was hitherto deemed necessary. We impose pN-forces on two fluid membranes, locally pre-adhered by RGD-integrin binding. One of the binding partners is always mobile whereas the mobility of the other can be switched on or off. Immediate passive strengthening of adhesion structures occurs in both cases. When both binding partners are mobile, strengthening is aided by lateral movement of intact bonds as a transient response to force-induced membrane-deformation. By extending our microinterferometric technique to the suboptical regime, we show that the adhesion, as well as the resistance to force-induced de-adhesion, is greatly enhanced when both, rather than only one, of the binding partners are mobile. We formulate a theory that explains our observations by linking the macroscopic shape deformation with the microscopic formation of bonds, which further elucidates the importance of receptor mobility. We propose this fast passive response to be the first-recognition that triggers signaling events leading to mechanosensing in living cells.

cell adhesion under force | dynamic reflection interference contrast microscopy | magnetic tweezers | mobile integrin-RGD bonds | model systems

The formation of adhesion domains is a ubiquitous event in the early stages of cell adhesion. The domains are agglomerates of bonds formed between receptors and counterreceptors (1). For cell–cell contact, before adhesion, both binding partners are mobile, whereas for cells adhering to the extracellular matrix, the counterreceptors are fixed. In the late, actively regulated stage of adhesion, the actin cytoskeleton couples to the adhesion domains (2). Under force, the adhesion domains grow (3) (a phenomenon called mechanoresponse, which is also related to mechanosensing, the ability of cells to sense and respond to rigidity) presumably by applying internal forces that interrogate the substrate (4). Force-induced strengthening is concomitant with the stiffening of the cytoskeleton (3, 5, 6), leading to the widespread belief that active regulation of the cytoskeleton is solely responsible for mechanoresponse (3, 5–9). However, this actively driven cytoskeletal remodeling due to external mechanical stimulus is expected to occur over time scales of minutes (4). Although it has been mooted previously that, at shorter time scales, the response is dominated by the physical properties of the membrane (1, 10), the force-response of cells over subsecond time scales has rarely been explored. At the same time, several studies have shown that, even in the absence of force, the adhesion is enhanced if both the ligands and the receptors mediating the binding are mobile (11, 12), in comparison with the case when only one of the binding partners diffuses in the membrane. Nevertheless, most recent experiments on mechanoresponse/sensing have been on cells adhering to a substrate decorated with immobilized receptors, the assumption being that receptor mobility does not seriously affect the force response. To explore the role of mobility and the response on short time scales, as well as to distinguish between passive and active effects, we constructed a clean cell-free model system where all of the parameters can be controlled and the observed effects can be attributed unequivocally to their source. The results emerging herein seriously challenge the assumptions discussed above.

Our model (11, 13) consists of a giant unilamellar vesicle with mobile RGD-peptide-carrying lipids (14), which interact with a supported bilayer doped with $\alpha_{IIb}\beta_3$ integrins (14). Depending on the specific deposition technique used (11, 13), the integrins are either fixed (immobile system; Fig. 1*a*) or exhibit in-plane mobility (mobile system; Fig. 1*b*). Because integrin mobility is the only difference between the two systems, the role of receptor-mobility can be clearly elucidated.

Studies on similar models (11, 13, 15–19) have contributed to understanding the initial stages of cell adhesion in the absence of force. The adhering vesicle assumes a truncated oblate shape where a given fraction of the membrane is parallel to the substrate forming a contact zone (Fig. 1). The size of the contact zone is defined by the vesicle-spreading pressure (change in free energy when decreasing the contact zone by a unit area). In the contact zone, strongly fluctuating membrane is interspersed with immobilized agglomerates (adhesion domains) of RGD–integrin bonds. In previous studies, the adhesion was promoted by domains that were, from the biological perspective, considerably oversized (18, 19). By using realistic, biologically relevant receptor concentrations, we ensure that the adhesion domains in the current system mimic the small micrometer- or sub-micrometer-sized focal-adhesion/focal-complexes found in cells. This realistic bond concentration accesses a regime of weak adhesion where bond-enthalpy competes with other contributions to the free energy, allowing for the rich response detailed in the remainder of the manuscript.

The technical challenge of identifying small as well as large but dilute bond clusters, typical for this system, is overcome by establishing the technique of dynamical reflection interference contrast microscopy (Dy-RICM). In traditional reflection interference contrast microscopy (RICM) (18–20), the height of the vesicle membrane above the substrate is determined and micrometer-sized domains with densely packed bonds are identified (11, 20). Dy-RICM exploits the vertical resolution of the set-up, which, at 5 nm, is an order of magnitude higher than the lateral resolution. The

Author contributions: A.-S.S., K.S., U.S., and E.S. designed research; A.-S.S. and S.G. performed research; A.-S.S. and K.S. analyzed data; and A.-S.S. and K.S. wrote the paper.

The authors declare no conflict of interest.

[‡]To whom correspondence should be addressed. E-mail: smith@theo2.physik.uni-stuttgart.de.

This article contains supporting information online at www.pnas.org/cgi/content/full/0801706105/DCSupplemental.

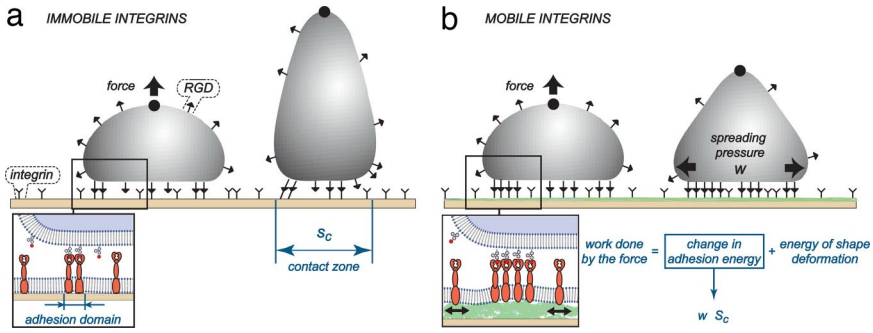

Fig. 1. Schematic presentation of two cell-mimetic model systems equilibrated in the absence and presence of a constant lifting force. (*a*) A giant unilamellar vesicle (DMPC:cholesterol:RGD-lipid:PEG2000 = 1:1:0.01:0.01 molar fraction) adheres to immobile integrins (100 integrins per mm^2) that are embedded in a DMPC:DMPG = 1:1 bilayer supported on glass. (*b*) A vesicle (DMPC:cholesterol:RGD-lipid:PEG2000 = 1:1:0.01:0.03) interacts with a mobile integrin-containing bilayer deposited on an ultra-thin layer of cellulose (100 integrins per mm^2). Although the systems are prepared with the same concentrations of RGD-lipids and integrins, in *b*, mobile integrins migrate into the contact zone between the vesicle and the bilayer producing more bonds and a larger spreading pressure w capable of opposing the force. Consequently, the same force creates smaller deformations and reduced loss of contact zone area in the mobile system.

technique is based on the construction of height-fluctuation maps, which show the mean fluctuation amplitude of each pixel in a time sequence [see details in supporting information (SI) *Text* and Figs. S1–S5]. Adhesion domains are identified as nonfluctuating regions in the contact zone. The threshold for identifying "adhesion" is set by the noise level, which, in turn, is determined from an analysis of the apparent height fluctuation in the background. By using Dy-RICM, it is possible to identify nanoscopic or dilute bond agglomerations and to follow their evolution to mature, micrometer-sized domains. By using traditional RICM to construct a snapshot of the topography of the entire contact zone, the mature domains are easily identified by choosing an appropriate cut-off height (here, 40 nm; refs. 21 and 22).

Upon the establishment of the adhesion equilibrium, a known, step-like force of 4 ± 2 pN was applied by vertical magnetic tweezers (20, 23) to a 2.25-μm paramagnetic bead covalently bound to the vesicle (see *SI Text* for details). The tweezers were developed specifically for these experiments (*SI Text* and Fig. S6) and imposed a constant force rather than a constant deformation (13). Subject to force, the vesicle membrane deforms and serves as a transmitter of the applied force to the bonds in the contact zone, which has a tendency to shrink (24). If the integrins are fixed on the substrate, the bonds at the edge of the contact zone respond by stretching and eventually break (Fig. 1*a*). To balance the elastic deformation, and the enthalpy of binding with the translational entropy of RGD, the system equilibrates under force by forming new bonds in the reduced contact zone of the strongly deformed vesicle. On the other hand, if the integrins are mobile (Fig. 1*b*), they too contribute to the entropy of the system. Instead of breaking, the bonds under force migrate into the contact zone, and thus build a larger spreading pressure, which in turn prevents large deformations of the vesicle shape. As a result, depending on the mobility of integrins, two very different scenarios of the force equilibration are observed as detailed in the remainder of the manuscript.

Detachment of RGD Vesicles

Immobile Integrins. In the immobile system (Fig. 1*a*), the low concentrations of RGD and integrin (10^3 and 10^2 molecules/μm^2, respectively) support only the formation of small domains (Fig. 2*a*). Although the distribution of integrins is uniform on the micrometer scale (11), spots of locally elevated integrin concentration occur. At these locations, more than one bond can be created simultaneously, and adhesion domains can form. Under force in the immobile system, the domains initially appear stable and pin the edge of the contact zone, which in turn forms sharp angles around the domains (Fig. 2*a*). The correspondence between the positions of the pinning points and the black regions in fluctuation maps confirms that these are indeed points of adhesion capable of opposing the force. However, the bonds at the edge are stretched, and the energy barrier governing bond rupture is decreased at the level of a single bond (25), making the domains more susceptible to force (26, 27) (Fig. 2*b*). The rupture of entire domains is accompanied by a fast local retraction of the membrane (500 ms for up to a couple of micrometers), which then gets pinned again at some preexisting or newly formed domain. The latter have been observed even in regions of the contact zone that were initially a few hundreds of nanometers above the substrate.

Under repeated pulling, the unbinding process in the immobile system is reversible in that it does not depend on the history of force application. The equilibrium size of the contact zone, both with and without force, is preserved in consecutive pulses, (Fig. 2*d*). Furthermore, when the vesicle respreads over the same part of the substrate upon release, a contact zone is formed that is remarkably similar to the initial one (Fig. 2*e*). The details of de-adhesion are also replicated for each force pulse and include domain formation at the same positions as well as a similar sequence of domain ruptures, simply because the distribution of immobile integrins on the substrate remains unperturbed (compare the two rows in Fig. 2*e*, which represent two consecutive force applications).

Because of formation of new domains and dynamic rebinding within the domains (26, 27), the spreading pressure is built, which in turn resists the force. A new equilibrium arises although with a significantly reduced contact zone (Fig. 2 *d* and *e*). This resistance is a direct consequence of the mobility of the RGD-lipids, and, as will be seen in the following section, additional mobility of integrins dramatically enhances the effect.

Mobile Integrins. In the mobile system (Fig. 1*b*), an entirely different scenario emerges. For the same concentrations of RGD-lipid and integrin as in the immobile system, the area associated with adhesion domains is an order of magnitude larger, indicating that considerably more bonds are formed (compare fluctuation maps in Fig. 3*a* with Fig. 2*a*) and some domains become visible in RICM (outlined in white in Fig. 3*a*). The increase of the equilibrium domain area at $f = 0$ is directly a consequence of the diffusion of mobile integrins into the contact zone.

In the mobile system, domains seldom rupture under force. Instead, during the first seconds of force application, intact bonds move laterally along with the edge of the contact zone toward proximate adhesion domains (Fig. 3*b*). This response indicates that the stretching of bonds is energetically more expensive than overcoming the opposing friction in both membranes (Fig. 3*c*). Bonds under force are brought closer together (e.g., the domain shrinks between t_1, and t_3 in Fig. 3*b*) leading to the appearance of a new

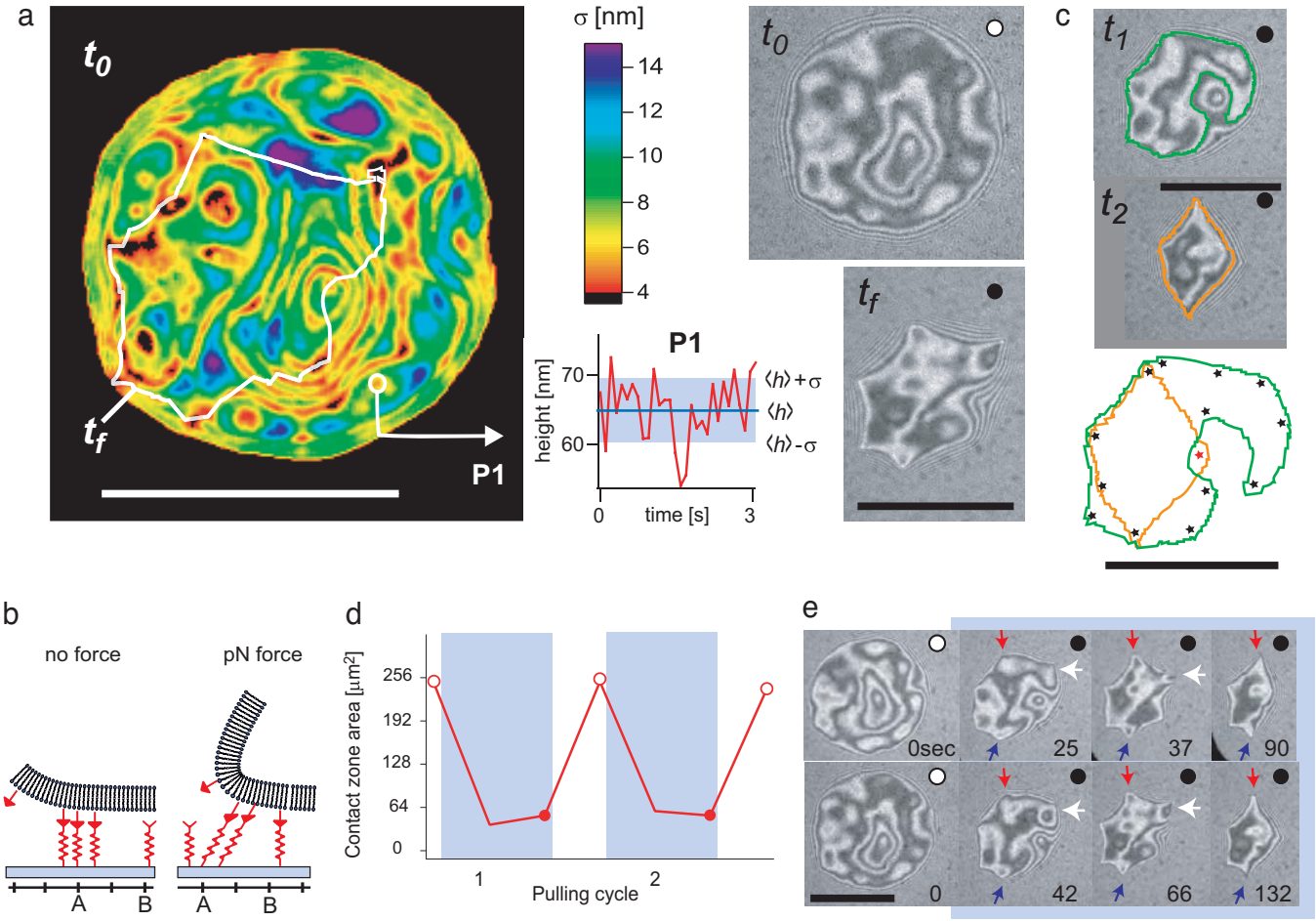

Fig. 2. Detachment of RGD-vesicles adhered to immobile integrins. (*a*) Comparison of the fluctuation map (*Left*) and the RIC-micrograph (*Top Right*) at t_0 and $f = 0$. Small black regions in the fluctuation map are assigned to adhesion domains although none could be identified in the RIC micrograph. The map is overlaid with the edge of the contact zone under force (white) at time t_f (RIC-micrograph; *Bottom Right*). The graph represents the height h of the vesicle membrane in a pixel P1 in a sequence of 30 consecutive frames. The mean height $<h>$ and the mean fluctuation amplitude s are indicated. Constructing a pixel-by-pixel chart of standard deviations s of h yields the fluctuation map. (*b*) Schematic representation of the domain response to the force. (*c*) The edge of the contact zone is first shown in two RIC-micrographs ($t_1 < t_2$) and then overlaid below. The adhesion domains are represented by stars. The red star indicates a newly formed domain seen at t_2 but not at t_1. (*d*) Area of the contact zone (error ≈ 1%) without and with force (shaded blue). (*e*) A similar sequence of domain formation and failure (≈50 per cycle) in two force cycles. Colored arrows point to three corresponding domains. Hollow dots, $f = 0$; filled dots, 4 pN. (Scale bar: 10 mm.)

domain in the RIC-micrograph (t_3 in Fig. 3*b*). These aggregates are stabilized by the force-induced membrane deformations and the suppression of fluctuations. They scatter away when the force is removed, showing that bonds do not spontaneously diffuse in the equilibrium. However, if a domain reaches a critical size of the order of 10^4 nm^2, the fluctuations act instead to stabilize the agglomerate (28). Irrespective of the force, the domain remains visible, both in the RICM and in the fluctuation map, and may grow during equilibration (Fig. 3*d*). Domains above this critical size are stationary, presumably because of the high frictional cost of displacing a large number of bonds simultaneously.

In the context of the detachment of the contact zone, equivalent constant forces are much less efficient in the mobile system than in the immobile system (contrast 25% area loss due to detachment seen in Fig. 3*e* with 75% in Fig. 2*d*). The more uniform initial distribution of bonds in the mobile system ensures that the boundary of the contact zone under force is mostly smooth and does not exhibit many pinned corners (contrast Figs. 3*d* and 2*d*). The resistance to the force is provided by both the displacement of existing bonds and the formation of new bonds, which in turn together build the spreading pressure.

If the force-induced change in the spreading pressure is large, upon release there is a transient excess pressure which induces enhanced spreading. Consequently, in a force cycle, the final zero-force contact zone is larger and has more bonds than the initial zero-force configuration (see t_1 and t_3 in Fig. 3*d*). The unbinding/rebinding sequence thus depends on the history of force application, and is therefore irreversible. The overall consequence is a sustained growth of both the contact zone (Fig. 3*e*) and the adhesion domains under repeated force cycles (Fig. 3*d*).

Statistical Elastic Theory and Discussion

The counterintuitive resistance to a detaching force seen in both systems, as well as the main differences between the two systems, namely the enhanced binding and growth under force seen in the mobile case, can be understood from a simple thermo-elastic theory for the equilibrium state of adhesion under force. The key element is the consideration of the competition between the tendency of the adhesion molecules to bind (thus gaining enthalpy), and the tendency to remain mobile (thus gaining entropy). Overall, the balance of these contributions results in a contact zone that is partially adhered, with bound and free ligands and receptors, as observed for the both mobile and immobile integrin cases. Further, in response to the force, the vesicle is deformed at the macroscopic scale, which

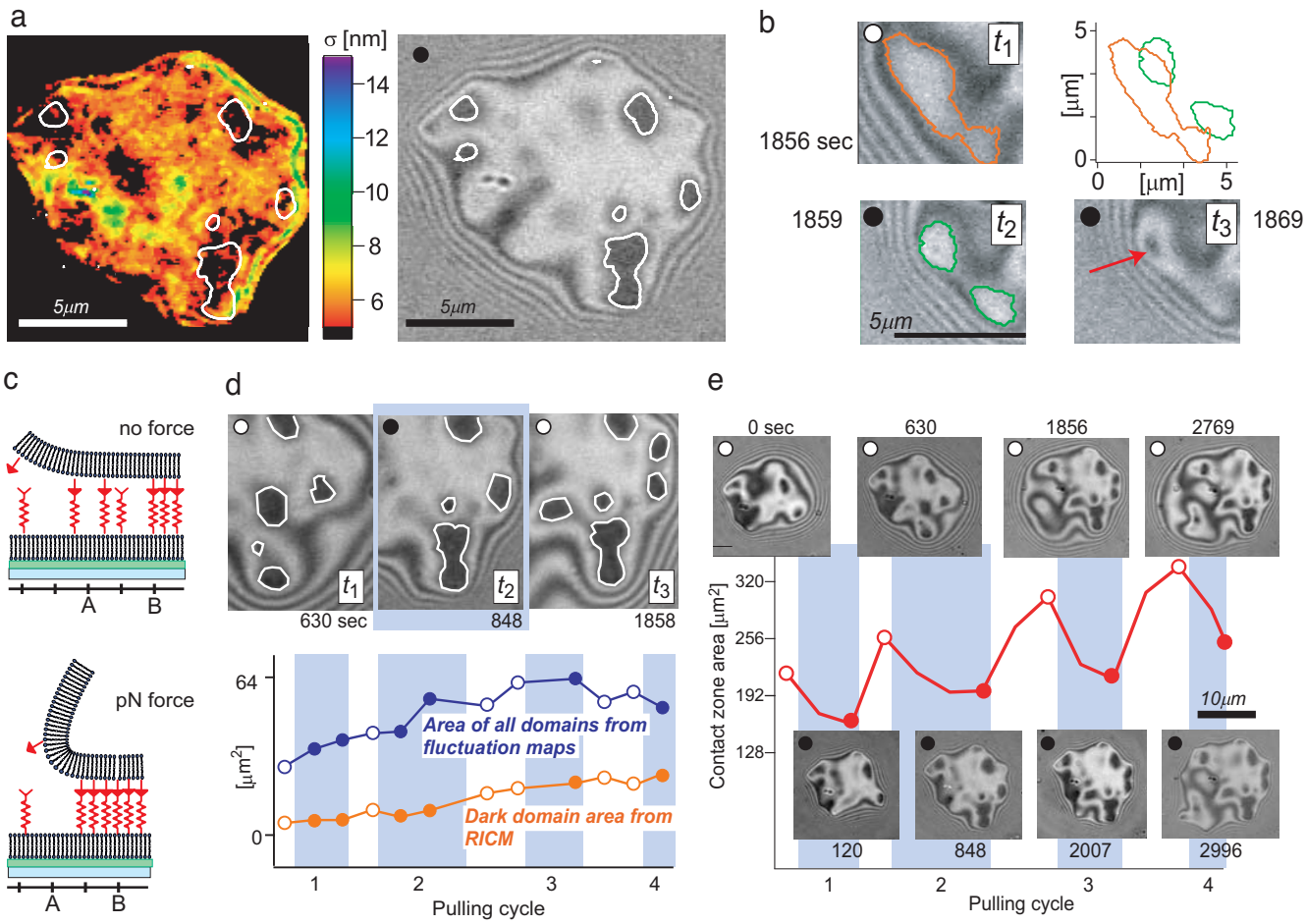

Fig. 3. Detachment of RGD-vesicles adhered to immobile integrins. (*a*) Large adhesion domains (enclosed in white and overlaid) in the RIC-micrograph (*Left*) are a fraction of the total domain area seen as black in the fluctuation map (*Right*). (*b*) Lateral displacement of an adhesion domain (enclosed in orange at t_1 and $f = 0$, and green at t_2 under $f = 4$ pN) is of the order of 2 mm and occurs over a transient time ($t_1 - t_2 = 3$ s). The same domain is immobilized and appears black at t_3 under force. (*c*) Schematic representation of the domain response to a force. (*d*) The growth of the total domain area and the dark domain area in four consecutive force cycles (error ≈ 20%). Domains seldom break (a total of six failures in four force cycles). Adhesion domains are outlined in white in the insets (respective entire micrographs shown in *e* with $f = 0$ (t_1, t_3), and $f = 4$ pN (t_2). (*e*) Consecutive equilibrium contact zones (average of 30 frames) in the absence of (*Upper*) and under force (*Lower*), showing the increase in the contact zone area (red curve; error ≈ 1%) between successive force applications.

in turn changes the spreading pressure (defined as the change in free energy when decreasing the contact zone by a unit area) and thus affects the numerous binding and unbinding events taking place in the contact zone. Together, these two concepts are the main ingredients for the theory built herein that explains the equilibrium behavior of the explored systems both in the presence and absence of force.

Building on previous work (24, 29–34), we construct a self-consistent model where the total free energy of the system F (in units of k_BT) consists of the elastic deformation energy (F_{elast}) of the vesicle under force, the binding energy of N_b formed bonds (each bond contributes E_a of binding energy), and the positional entropy of mobile RGD-lipids and integrins:

$$F = F_{\text{elast}} - N_{\text{b}}E_{\text{a}} - \sum_{i=1}^{4} \ln\Omega_{\text{i}}, \qquad [1]$$

where Ω_i represent all of the possible positional configurations. The elastic term consists of contributions from (*i*) the elastic shape deformation (giving rise to the bending energy F_{bend}) induced by a vertical displacement of the apex of the vesicle Δh under force f, and (*ii*) the spreading pressure w produced by the bonds ($w = -\text{d}F/\text{d}S_{\text{c}}$) in the contact zone of area αS_{c} (a is the area of a unit site and S_{c} is the number of sites in the contact zone):

$$F_{\text{elast}} = F_{\text{bend}} + f\Delta h - \frac{dF}{dS_{\text{c}}} aS_{\text{c}}. \qquad [2]$$

To determine the shape of the vesicle (including the size of the contact zone), and the number of free and bound integrins, this equation must be solved self-consistently with Eq. **1** under constraints on the total area and volume of the vesicle (24, 31). In the absence of applied force, the balance between the spreading pressure (which is equal to the adhesion energy density in homogeneously adhering vesicles) and the elastic energy of deformation due to adhesion determines the shape. Application of force results in a reduction of the size of the contact zone (24), both in the immobile and the mobile case. An example of the calculated shape of the vesicle in presence of force is shown in Fig. 1.

The enthalpic contribution (second term on the right hand side) in Eq. **1** is obtained by counting the number of formed bonds N_{b}. A bond is formed with a certain probability whenever an RGD in a vesicle is positioned above an integrin on the substrate. In the present approach, the probability for bond formation is set to one (assigning a probability less then one is equivalent to rescaling the

binding affinity of a single bond, because the probability enters as a prefactor of the enthalpy term in Eq. **1**). Furthermore, applying a constant force, in Kramer's picture, changes the effective potential at the level of a single bond by adding a constant contribution (30). Binding and unbinding rates in this case depend on the force, but do not evolve with time. In effect, this means that the effective binding affinity is slightly different in the presence and absence of force. In the current case, the total applied force is very small and is distributed over many bonds (constant 4 pN applied to the membrane, which distributes among $\approx 10^4$ bonds in the contact zone). The loading rate too is relatively low and is transient (it takes a few microseconds for the force to step from 0 to 4 pN). Furthermore, only the bonds at the edge of the contact zone feel the load directly whereas the bonds in the interior of the contact zone provide a thermodynamic response that determines the spreading pressure. In the equilibrium states analyzed herein, which are established after the bonds at the edge have failed (in the immobile system) or migrated (mobile system) to the region where the substrate and the vesicle membrane are parallel, all bonds present participate in the thermodynamic response. Changing the bond strength at this stage, ultimately changes the number of bonds in the system but does not change the tendency of increased bond density in response to a decrease of the contact zone area (see *SI Text* and Fig. S7, for results with a larger binding affinity). Even so, such a change in bond strength in the current system can be expected to be very small because of the small force imposed. Thus, we are justified in our approximation of a constant binding affinity that is force independent.

The entropic contribution (last term on the right hand side) to the energy in Eq. **1** is obtained by considering a vesicle discretized to S_t sites (S_t = total surface area/the area occupied by a single RGD-lipid). The total number of RGDs in a vesicle is T_{RGD}. Some of these (N_{RGD}) reside in the contact zone. To adhere, the vesicle forms a contact zone with the substrate (spanning S_c sites out of S_t). In contrast to the constant total number of RGDs in the vesicle, the mobile integrins reside on a virtually infinite bilayer and are thus coupled to a reservoir of a constant bulk concentration ρ_{bulk}. A certain number of integrins N_i are in the contact zone, and their density is $n_i = N_i/S_c$. For mobile integrins, n_i is not known and must be determined simultaneously with the number of formed bonds. For immobile integrins, $n_i = \rho_{bulk}$ (24, 29).

In the spirit of the mixing entropy concept but for a finite vesicle system, the entropy term can be explicitly written as:

$$\Omega = \Omega_1\Omega_2\Omega_3\Omega_4 = \binom{S_c}{N_i - N_b}\binom{S_c - N_i}{N_{RGD} - N_b}\binom{N_i}{N_b}\binom{S_t - S_c}{T_{RGD} - N_{RGD}}. \quad [3]$$

Here, the terms of the form $\binom{A}{B}$ indicate the number of ways in which B objects can be arranged on A sites (see *SI Text* for details). Written in this form, the entropy is defined within a finite constrained geometry, which is a key to the establishment of a new equilibrium under force. Thereby, Ω_1 and Ω_2, account for the mobility of nonbound integrins and nonbound RGDs within the contact zone, respectively. Because the immobile integrins do not contribute to the entropy, $\Omega_1 = 1$ (24, 29). Ω_3 accounts for the rearrangement of bonds by the unbinding and rebinding of RGDs to integrins, but maintaining the total number of bonds fixed. Ω_4 accounts for the RGDs outside of the contact zone. In the mobile system, experiments show that, although bonds move during equilibration under force, the frictional coupling between the two membranes considerably decreases the diffusion of bonds in equilibrium. Therefore, Eq. **3** does not contain a contribution from laterally mobile bonds.

It has been shown that, because of the very different scales involved, the equilibration of the vesicle shape and that of the bonds in the contact zone are decoupled (20). Thus, the area of the contact zone can be treated as a parameter imposed by the applied force and the properties of the vesicle-substrate system (e.g., the membrane bending stiffness and adhesion energy). Accordingly, the last two terms in Eq. **1** can be treated separately from (but consistently with) the shape determination. For a given size of the contact zone, the optimum solution for the number of formed bonds results from numerically solving $\partial F/\partial N_b = \partial F/\partial N_f = 0$ and $\partial F/\partial S_r = \ln\rho_r^{bulk}$. The last equation couples the receptors in the contact zone to the reservoir of constant chemical potential with a constant density of receptors ρ_r^{bulk}. The number of RGDs in a vesicle is fixed and finite.

Minimization of Eq. **1**, using standard numerical procedures (see *SI Text*) provides the density of free integrins and formed bonds as a function of the contact zone size (Fig. 4*a*).

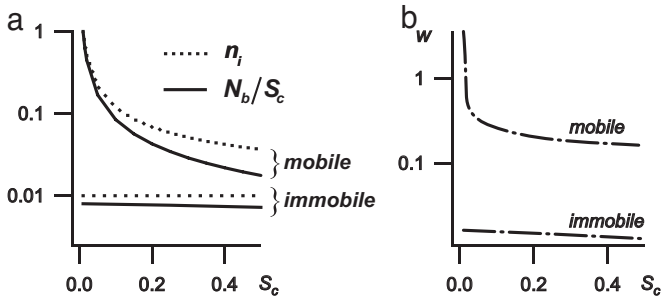

Fig. 4. Theoretical analysis of the role of integrin-mobility. (*a*) The density of integrins $n_i = N_i/S_c$ (dotted line) and the density of formed bonds N_b/S_c (solid line) as a function of the size of the contact zone s_c (normalized by the total area of the vesicle, $s_c = S_c/A$) is calculated to be much larger in case of mobile than immobile integrins. When under force, the contact zone becomes smaller and the solutions for the corresponding increasing receptor-density and bond-density are found by moving leftward along the plotted lines. (*b*) The spreading pressure w as a function of the size of the contact zone increases monotonically when S_c decreases (in response to the force). Experimentally relevant parameters are chosen: $E_a = 6\ k_BT$, 1% integrin and RGD surface coverage, and a vesicle diameter of 20 mm. The trends are robust under changes in the parameter values (*SI Text* and Fig. S7).

The theoretical results confirm that, even in the absence of force, mobile integrins migrate into the contact zone and increase the probability of bond formation. Therefore, the number of bonds formed in the mobile system is predicted to be a couple of orders of magnitude higher than in the immobile system. In both systems, the vesicle attains a stable state with as many bonds formed as is possible for the given size of the contact zone.

The exact dependence of the number of bonds on the size of the contact zone is sensitive to the densities of the RGD and integrin, and to their mutual binding affinity. The magnitude of these dependencies is less pronounced in the mobile integrin case because the number of integrins in the contact zone cannot be modulated and thus the balance between the entropy and enthalpy is less amenable to adjustment. In all cases, an attempt to decrease the contact zone results in a net decrease of the total number of bonds. However, the remaining bonds reorganize or redistribute in such a way that their density increases. Thus, for a sufficiently small contact zone, most integrins therein are bonded. In the mobile case, the density of bonds in the contact zone should eventually reach unity when the entire contact zone is filled with the receptors (for the parameters in Fig. 4, $n_i = 1$ for $s_c \leq 0.01$). In the immobile system, on the other hand, the density of integrins is imposed *a priori*. Only in the limit of zero binding affinity, the density is constant and the spreading pressure is insensitive to the size of the contact zone. At the other limit of large binding affinities, and at large concentrations of RGD, all of the available integrins are expected to be bound. Even at this limit of integrin saturation, irrespective of the mobility, a reduction in the contact zone area leads to an increase in the spreading pressure purely due to entropic

reasons (24, 29). However, in the current system, the low concentration of RGD ensures that this limit is not reached, a fact confirmed both by the experiments and the results of the calculations. In this case, as in all cases away from the zero binding affinity limit, the spreading pressure is determined by a balance of entropy and enthalpy and increases with a decrease in contact zone size (24, 29) (Fig. 4*b*).

In terms of the spreading pressure, under force, a new stable state is achieved when the tendency of the force to decrease the contact-zone size is balanced by the increase in the spreading pressure. The applied force thus determines the size of the contact zone and the shape of the vesicle. Larger and larger forces must be used to make the contact zone smaller and smaller, a fact valid in both systems. However, the larger and more variable spreading pressure possible in the mobile system leads to the experimentally verified expectation that smaller detachment of the contact zone and smaller deformations of the vesicle shape should be observed in the case of mobile integrins (as shown in Fig. 1).

Upon release of the force, in the immobile case, the vesicle returns to its initial state. However, in the mobile case, application of force increases the number of bonds in the contact zone and the spreading pressure much more drastically (Fig. 4). Upon release of the force, this transiently excess spreading pressure drives the vesicle into a new stable state, which is a new balance between the elastic deformation and the spreading pressure. This new state is closer to the global energy minimum and corresponds to a larger contact zone and a larger adhesion area. Repeated force cycles thus drive the system toward enhanced adhesion.

In conclusion, we have shown that the theoretically expected strengthening of the adhesion domains under force clearly occurs in analogous experimental situations. Because this effect arises from general principles and does not depend on specific proteins, a similar mechanism is expected to be present in all cell membranes and may play a role in the mechanoresponse of living cells. Indeed, it has been previously demonstrated both in mimetic systems (35) and in motile cells (36) that application of force leads to simultaneous decrease in the contact zone area and increase in the adhesion energy density (which, in our system, is equivalent to an increase in the spreading pressure). Furthermore, it has also been shown that, in these cells, reduction of ligand mobility greatly decreases the adhesion strengthening under force (12). Our in-depth analysis of the events occurring in the contact zone demonstrates that all these observations can be understood in a unified manner by considering, in addition to the elastic response of the membrane, the interplay between entropy of the free receptors and enthalpy of bond formation.

Because this passive strengthening and *ab initio* formation of domains under force occurs on time scales that are considerably faster than the active cytoskeletal response, we see it as a strong candidate for the elusive force-sensor (3–8), which triggers the activation of signaling pathways leading to force-dependent regulation of adhesion in living cells. This passive sensing requires only an intact cell membrane with mobile adhesion proteins and should be noticeable even before proper focal adhesions or stress-fibers are formed, which indeed seems to be the case, not only in the motile cells capable of rapid adhesion and translation (36) but also in focal-adhesion forming cells (4). The consequences of the different ways in which bonds involving immobile and mobile receptors respond to the force (bond-stretching versus bond-displacement), leading to different response-mechanisms in the model systems, are yet to be investigated fully in the cellular context. Our results suggest that, owing to differences in the mobility of the binding partners, mechanosensing should be more significant in cell–cell adhesion than in cell–matrix adhesion. We anticipate that the general physical principles set out here and tested in a model system will initiate experiments that can identify this phenomenon in living cells.

ACKNOWLEDGMENTS. We benefited from discussions with K. R. Mecke and R. Merkel. We thank D. Smith and L. Limozin for critical reading of the manuscript. We thank the referees for pointing out key references that demonstrate the validity of our predictions in living cells. This work was supported by Sonderforschungsbereich Grant 563-C4 (to S.G. and E.S.) and by Deutsche Forschungsgemeinschaft Grant SE 1119/2-1 (to A-S.S.).

1. Pierres A, Benoliel A, Bongrand P (2000) Cell–cell interactions. *Physical Chemistry of Biological Interfaces*, eds Norde W, Baszkin A (Marcel Dekker, New York) pp 459–522.
2. Zimerman B, Volberg T, Geiger B (2004) Early molecular events in the assembly of the focal adhesion-stress fiber complex during fibroblast spreading. *Cell Motil Cytoskel* 58:143–159.
3. Balaban NQ, *et al*. (2001) Force and focal adhesion assembly: A close relationship studied using elastic micropatterned substrates. *Nat Cell Biol* 5:466–472.
4. Bershadsky A, Kozlov M, Geiger B (2006) Adhesion-mediated mechanosensitivity: A time to experiment, and a time to theorize. *Curr Opin Cell Biol* 18:472–481.
5. Polte TR, Eichler GS, Wang N, Ingber DE (2004) Extracellular matrix controls myosin light chain phosphorylation and cell contractility through modulation of cell shape and cytoskeletal prestress. *Am J Physiol Cell Physiol* 286:C518–C528.
6. Micoulet A, Spatz JP, Ott A (2005) Mechanical response analysis and power generation by single-cell stretching. *ChemPhysChem* 6:663–670.
7. Bruinsma R (2005) Theory of force regulation by Nascent adhesion sites. *Biophys J* 89:87–94.
8. Besser A, Safran SA (2006) Force-induced adsorption and anisotropic growth of focal adhesions. *Biophys J* 90:3469–3484.
9. Tzima E, *et al*. (2005) A mechanosensory complex that mediates the endothelial cell response to fluid shear stress. *Nature* 437:426–431.
10. Grabovsky V, *et al*. (2000) Subsecond induction of alpha 4 integrin clustering by immobilized chemokines stimulates leukocyte tethering and rolling on endothelial vascular cell adhesion molecule 1 under flow conditions. *J Exp Med* 192:495–505.
11. Goennenwein S, Tanaka M, Hu B, Moroder L, Sackmann E (2003) Functional incorporation of integrins into solid supported membranes on ultrathin films of cellulose: Impact on adhesion. *Biophys J* 85:646–655.
12. Chan PY, *et al*. (1991) Influence of receptor lateral mobility on adhesion strengthening between membranes containing LFA-3 and CD2. *J Cell Biol* 115:245–255.
13. Goennenwein S (2003) Generic and specific cell adhesion: Investigations of a model system by micro-interferometry. PhD Thesis (Technische Universität, Munich).
14. Hu B, *et al*. (2000) Intervesicle cross-linking with integrin alpha(IIb)beta(3) and cyclic-RGD-lipopeptide: A model of cell-adhesion processes. *Biochemistry* 39:12284–12294.
15. Lenz P, Ajo-Franklin CM, Boxer SG (2004) Patterned supported lipid bilayers and monolayers on poly(dimethylsiloxane). *Langmuir* 20:11092–11099.
16. Liu AP, Fletcher DA (2006) Actin polymerization serves as a membrane domain switch in model lipid bilayers. *Biophys J* 91:4064–4070.
17. Kahya N, Brown DA, Schwille P (2005) Raft partitioning and dynamic behavior of human placental alkaline phosphatase in giant unilamellar vesicles. *Biochemistry* 44:7479–7489.
18. Rädler J, Sackmann E (1993) Imaging optical thicknesses and separation distances of phospholipid-vesicles at solid-surfaces. *J Phys II* 3:727–748.
19. Cuvelier D, Nassoy P (2004) Hidden dynamics of vesicle adhesion induced by specific stickers. *Phys Rev Lett* 93:228101.
20. Smith A–S, Lorz BG, Goennenwein S, Sackmann E (2006) Force-controlled equilibria of specific vesicle-substrate adhesion. *Biophys J* 90:L52–L54.
21. Sengupta K, Aranda-Espinoza H, Smith L, Janmey P, Hammer D (2006) Spreading of neutrophils: From activation to migration. *Biophys J* 91:4638–4648.
22. Smith A–S, Lorz BG, Seifert U, Sackmann E (2006) Antagonist-induced deadhesion of specifically adhered vesicles. *Biophys J* 90:1064–1080.
23. Limozin L, Roth A, Sackmann E (2005) Microviscoelastic moduli of biomimetic cell envelopes. *Phys Rev Lett* 95:178101.
24. Smith A–S, Seifert U (2007) Vesicles as a model for controlled (de-) adhesion of cells: A thermodynamic approach. *Soft Matter* 3:275–289.
25. Merkel R, Nassoy P, Leung A, Ritchie K, Evans E (1999) Energy landscapes of receptor-ligand bonds explored with dynamic force spectroscopy. *Nature* 379:50–53.
26. Seifert U (2002) Dynamic strength of adhesion molecules: Role of rebinding and self-consistent rates. *Europhys Lett* 58:792–798.
27. Erdmann T, Schwarz US (2004) Stability of adhesion clusters under constant force. *Phys Rev Lett* 92:108102.
28. Zuckerman DM, Bruinsma R (1995) Statistical-mechanics of membrane adhesion by reversible molecular-bonds. *Phys Rev Lett* 74:3900–3903.
29. Smith A–S, Seifert U (2005) Effective adhesion strength of specifically bound vesicles. *Phys Rev E* 71:61902.
30. Bell GI, Dembo M, Bongrand P (1984) Cell-adhesion: Competition between nonspecific repulsion and specific bonding. *Biophys J* 45:1051–1064.
31. Seifert U, Lipowsky R (1990) Adhesion of vesicles. *Phys Rev A* 42:4768–4771.
32. Brochard-Wyart F, de Gennes PG (2002) Adhesion induced by mobile binders: Dynamics. *Proc Natl Acad Sci USA* 99:7854–7859.
33. Shenoy VB, Freund LB (2005) Growth and shape stabillity of a biological membrane adhesion complex in the diffusion-mediated regime. *Proc Natl Acad Sci USA* 102:3213–3218.
34. Freund LB, Lin Y (2004) The role of binder mobility in spontaneous adhesive contact and implications for cell adhesion. *J Mech Phys Solids* 52:2455–2472.
35. Maier CW, Behrisch A, Kloboucek A, Simson DA, Merkel R (2001) Specific biomembrane adhesion: Indirect lateral interactions between bound receptor molecules. *Euro Phys J E* 6:273–276.
36. Tozeren A, Sung KLP, Chien S (1989) Theoretical and experimental studies on cross-bridge migration during cell disaggregation. *Biophys J* 55:479–487.